Dynamic force spectroscopy of DNA hairpins: II. Irreversibility and dissipation

J. Stat. Mech. (2009) P02061

(http://iopscience.iop.org/1742-5468/2009/02/P02061)

Journal of Statistical Mechanics: Theory and Experiment
An IOP and SISSA journal

Dynamic force spectroscopy of DNA hairpins: II. Irreversibility and dissipation

M Manosas[1,3], A Mossa[1], N Forns[1,2], J M Huguet[1] and F Ritort[1,2]

[1] Departament de Física Fonamental, Facultat de Física, Universitat de Barcelona, Diagonal 647, E-08028 Barcelona, Spain
[2] CIBER-BBN Networking Center on Bioengineering, Biomaterials and Nanomedicine, Spain
E-mail: mmanosas@gmail.com, alessandro.mossa@gmail.com, nuforns@ub.edu, johuca@yahoo.com and ritort@ffn.ub.es

Received 9 December 2008
Accepted 12 January 2009
Published 25 February 2009

Online at stacks.iop.org/JSTAT/2009/P02061
doi:10.1088/1742-5468/2009/02/P02061

Abstract. We investigate irreversibility and dissipation in single molecules that cooperatively fold/unfold in a two-state manner under the action of mechanical force. We apply path thermodynamics to derive analytical expressions for the average dissipated work and the average hopping number in two-state systems. It is shown how these quantities only depend on two parameters that characterize the folding/unfolding kinetics of the molecule: the fragility and the coexistence hopping rate. The latter has to be rescaled to take into account the appropriate experimental set-up. Finally we carry out pulling experiments with optical tweezers in a specifically designed DNA hairpin that shows two-state cooperative folding. We then use these experimental results to validate our theoretical predictions.

Keywords: fluctuations (theory), fluctuations (experiment), mechanical properties (DNA, RNA, membranes, bio-polymers) (theory), mechanical properties (DNA, RNA, membranes, bio-polymers) (experiment)

[3] Present address: Laboratoire de Physique Statistique, Ecole Normale Supérieure, Unité Mixte de Recherche 8550 associée au Centre National de la Recherche Scientifique et aux Universités Paris VI et VII, 24 Rue Lhomond, F-75231 Paris, France.

1742-5468/09/P02061+28$30.00

Contents

1. Introduction

One of the most exciting aspects of single-molecule techniques is the possibility of accurately measuring tiny amounts of energy down to a tenth of a k_BT (at room temperature 1 k_BT corresponds to approximately 4 pN nm which is of the order of 10^{-21} J) [1]. The possibility of measuring such small energies opens new perspectives in the exploration of the properties and behavior of biological matter at both the cellular and molecular levels. Questions such as irreversibility, dissipation and energy fluctuations have received a new boost under the heading of *nonequilibrium thermodynamics of small systems*, a discipline that successfully combines theory and experiment and uses individual biomolecules as models to investigate the energetics of complex systems [2, 3].

This paper is a continuation of a companion one where we investigated in detail questions related to the thermodynamics and kinetics of simple two-state hairpins under applied force [4]. Here we investigate issues related to irreversibility and dissipation in pulling experiments of DNA hairpins that fold/unfold under the action of mechanical force. In these experiments the molecule is repeatedly unfolded/folded by increasing/decreasing

J. Stat. Mech. (2009) P02061

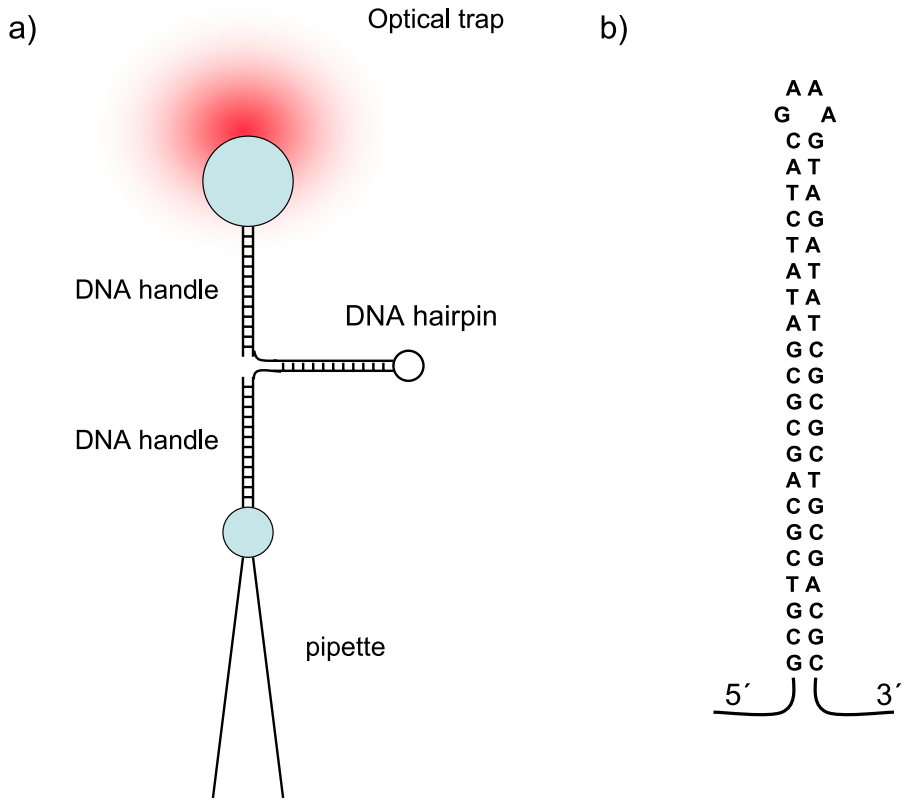

Figure 1. (a) Experimental set-up. (b) DNA sequence.

the force at a given pulling rate in a controlled way. The output of such experiments is the force–distance curve (FDC), a diagram that shows the force as a function of the trap position. We have carried out experiments (experimental set-up shown in figure 1(a)) using a high stability newly designed miniaturized dual-beam optical tweezers' apparatus [5] to pull a specifically designed DNA hairpin sequence (figure 1(b)). The specific sequence shows a simple two-state free energy landscape, ideal to compare theory and experiment [4]. We use the recently introduced theoretical approach of path thermodynamics [3, 6] to investigate questions related to the irreversibility and energy dissipation in two-state systems. The study of DNA hairpins [7] has advantages compared to RNA studies because the former degrades much slower than RNA does. This makes DNA an excellent model to address physics-related questions.

The content of this paper is divided into two main parts: the first part is mainly theoretical and describes the analytical results; the second part presents the experimental results and compares them with the theoretical predictions. The paper ends with some conclusions followed by a few appendices that include some technical aspects of the analytical computations.

2. Mechanical work, hopping number and free energy landscapes: a short reminder

We consider a pulling cycle (Γ) consisting of a stretching (S) and a releasing (R) part. In the stretching part the force is increased from a low force $f_{\min}$, where the hairpin is

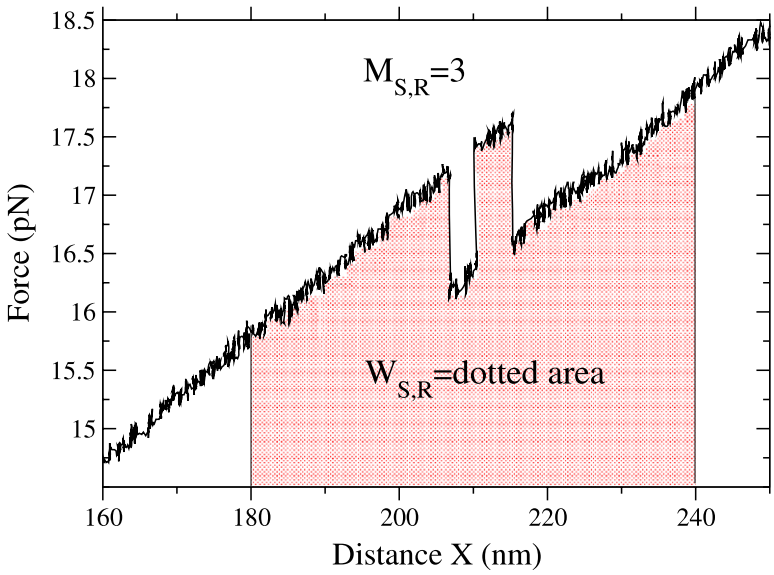

Figure 2. A representative FDC corresponding to either a stretching or releasing part of a cycle. It shows the relevant quantities that we investigate: the mechanical work exerted on the molecule $W_{\mathrm{S(R)}}$ (shown as the dotted area); and the number of transitions the molecule executes between the two states, $M_{\mathrm{S(R)}}$ (=3 in the example of the figure).

always folded, to a high force $f_{\max}$, where the hairpin is always unfolded. In the releasing part the force is decreased from $f_{\max}$ back to $f_{\min}$. To quantify irreversibility and energy dissipation during the stretching and releasing parts of the cycle, we introduce the two following quantities.

- *The mechanical work* $W_{\mathrm{S(R)}}$. The mechanical work $W_{\mathrm{S(R)}}$ along the stretching (releasing) part of the cycle Γ is the area below the FDC between the positions $X_{\min}$ and $X_{\max}$ (corresponding to the previously defined forces $f_{\min}$ and $f_{\max}$ along the FDC). It is defined by

$$W_{\mathrm{S(R)}}(\Gamma) = \int_{X_{\min}}^{X_{\max}} \mathrm{d}X\, F_{\mathrm{S(R)}}(X), \tag{1}$$

  where the subscript S(R) refers to the stretching (releasing) part of the cycle. Throughout this work we will take W_{S} and W_{R} as positive and negative quantities, respectively, although, according to (1), both have positive signs. In fact, the work in the S part of the cycle is performed by the instrument on the system ($\mathrm{d}X > 0$) whereas in the other case (R) the work is returned by the system to the instrument ($\mathrm{d}X < 0$). Figure 2 shows how we measure the work along a given FDC.
- *The hopping number* $M_{\mathrm{S(R)}}$. The hopping number $M_{\mathrm{S(R)}}$ along the stretching (releasing) part of the cycle Γ is the number of transitions or jumps (corresponding to force rips) that the molecule executes during the stretching (releasing) part of the cycle. $M_{\mathrm{S(R)}}$ can take only odd values $(1, 3, 5, \ldots)$ for all paths Γ performed between $f_{\min}$ and $f_{\max}$. An illustration is shown in figure 2.

doi:10.1088/1742-5468/2009/02/P02061

J. Stat. Mech. (2009) P02061

These are the main quantities that we will focus on in this paper. Out of the total work $W^{\mathrm{S(R)}}$ we can also extract, for each cycle Γ, the dissipated work $W_{\mathrm{dis}}^{\mathrm{S(R)}}$ which is equal to the difference between the work and the reversible work. The reversible work can be estimated either using the Jarzynski equality along the S(R) process [8] or the Crooks fluctuation relation [9, 10]. The latter combines measurements from both the S and R processes and provides better estimates for free energy differences. The Crooks fluctuation relation has been applied to recover the free energy of the DNA sequence shown in figure 1(b) (see our companion paper [4]).

The mechanical folding and unfolding of small nucleic acid (DNA or RNA) hairpins is commonly described with a two-state model [11]–[15]. In this model the hairpin can adopt two conformations or states, the folded (hereafter referred to as F) and the unfolded or stretched (hereafter referred to as UF) state. When subject to force, the projection x of the molecular extension along the force axis is an adequate reaction coordinate for the folding–unfolding reaction. For a given applied force f, the two-state approach considers a single kinetic pathway for the unfolding/folding reactions and the free energy landscape is characterized by a single transition state (hereafter referred to as TS). The TS is the state with highest free energy along the reaction coordinate and determines the kinetics of the unfolding (folding) reaction. The simplest version of the Kramers–Bell model (see [4] for details) is schematically depicted in figure 3(a). It involves only four parameters: the free energy difference ΔG_1, the kinetic barrier B_1 and the distances x^{F} and x^{UF} along the reaction coordinate axis that separates the TS from the F and UF states, respectively. The total distance between the F and U states will be denoted as x_{m} and can be written as $x_{\mathrm{m}} = x^{\mathrm{F}} + x^{\mathrm{UF}}$.

Two-state folders are well described by the so-called simplified Kramers–Bell kinetic rates:

$$k_{\rightarrow}(f) = k_{\mathrm{m}} \exp{(\beta f x^{\mathrm{F}})}, \qquad k_{\leftarrow}(f) = k_{\mathrm{m}} \exp{(\beta(\Delta G_1 - f x^{\mathrm{UF}}))}, \tag{2}$$

with $\beta = 1/k_{\mathrm{B}}T$, T being the temperature of the environment and k_{B} the Boltzmann constant. k_{m} corresponds to the unfolding rate at zero force and is given by $k_{\mathrm{m}} = k_0 \exp -(\beta B_1)$, where k_0 is an attempt frequency describing microscopic oscillations and effects of the experimental set-up (bead motion, fluctuations in extension of handles and ssDNA) and B_1 is the kinetic barrier. The parameter ΔG_1 in (2) is related to the total free energy difference between the F and UF states at force f: $\Delta G(f) = \Delta G_1 - f x_{\mathrm{m}}$. ΔG_1 gets contributions from the free energy of formation of the hairpin at zero force, ΔG_0, and the free energy of stretching the ssDNA up to the total extension x_{m} ($=x^{\mathrm{F}} + x^{\mathrm{UF}}$) at force f.

Equation (2) defines the coexistence force f_{c} where both rates are equal, $k_{\rightarrow}(f_{\mathrm{c}}) = k_{\leftarrow}(f_{\mathrm{c}})$, giving $f_{\mathrm{c}} = \Delta G_1/x_{\mathrm{m}}$. All parameters entering into the simplified rates (2) (i.e. k_{m}, x^{F}, x^{UF}, ΔG) are taken to be independent of force and ΔG_1 is evaluated at the critical force f_{c} (see [4] for a thorough discussion).

The distances $x^{\mathrm{F}}, x^{\mathrm{UF}}$ characterize how much the molecule deforms before unfolding. It is common to define the fragility parameter μ [18]–[21]:

$$\mu = \frac{x^{\mathrm{F}} - x^{\mathrm{UF}}}{x^{\mathrm{F}} + x^{\mathrm{UF}}}. \tag{3}$$

μ lies in the range $[-1 : 1]$ and defines the degree of compliance of the molecule under the effect of tension. Fragile or compliant molecules are those in which x^{F} is larger than x^{UF}

J. Stat. Mech. (2009) P02061

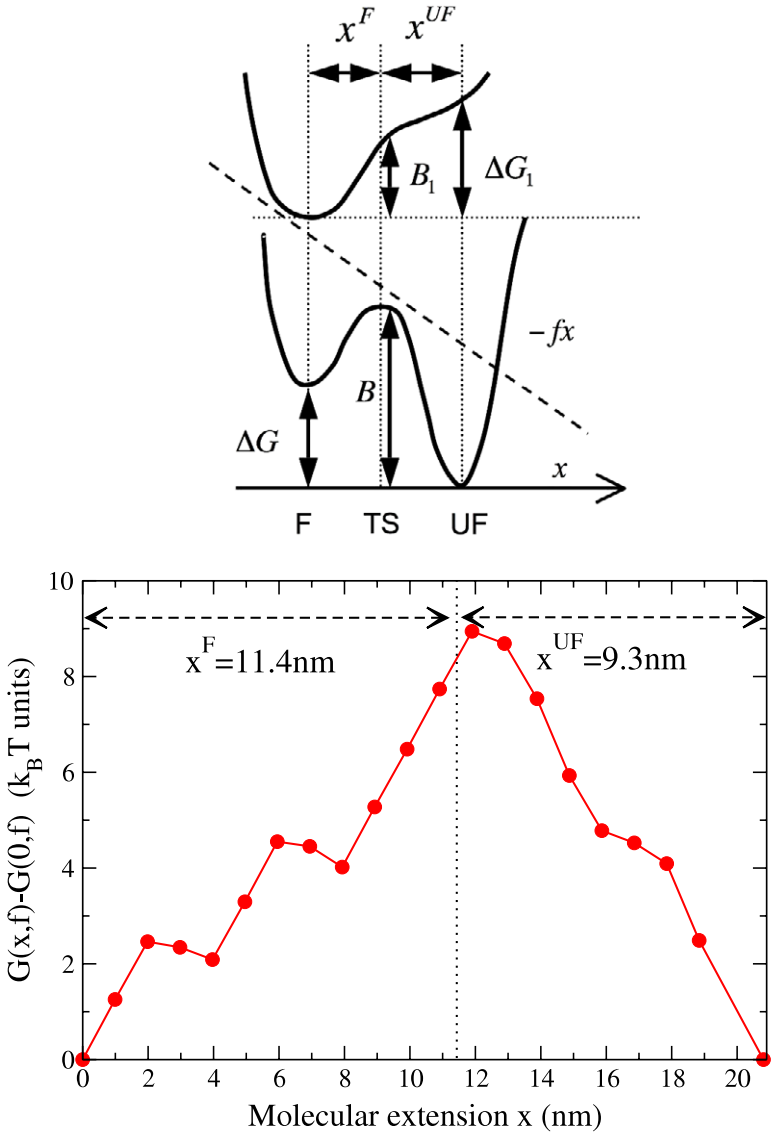

Figure 3. (Upper panel) Schematic picture of the two-state model. The free energy landscape of the molecule along the reaction coordinate axis x has two minima corresponding to the F and UF states. These states have free energies $G_{\rm F}$ and $G_{\rm UF}$ with $\Delta G = G_{\rm UF} - G_{\rm F}$. The two states (F and UF) are separated by the transition state (TS) that has a free energy B higher than that of the F state. The TS is located at distances $x^{\rm F}$ and $x^{\rm UF}$ from the F and UF states, respectively. When a mechanical force is applied to the ends of the molecule the free energy landscape is tilted along x, decreasing the free energy of the UF state and the TS relative to the F state. This induces a variation of B and ΔG which, in the simplified Kramers–Bell picture, are given by $B = B_1 - fx^{\rm F}; \Delta G = \Delta G_1 - fx_{\rm m}$, where $B_1, \Delta G_1$ are constant free energy parameters. (Lower panel) Free energy landscape $G(x, f)$ for the DNA hairpin shown in figure 1(b) plotted as a function of the number of open base pairs at $f = 17.9$ pN (buffer conditions are 1 M NaCl and 23 °C). The landscape has been calculated using the nearest-neighbor model [16] for thermodynamics using the free energy parameters given by Mfold [17] and the theory developed in [4].

J. Stat. Mech. (2009) P02061

and μ is positive. In contrast, when $x^{\rm UF}$ is larger than $x^{\rm F}$ and μ is negative we speak of brittle structures.

3. Mechanical work and hopping number in path thermodynamics

In this section we apply path thermodynamics [3] to find analytical expressions for the average dissipated work and the average hopping number in two-state systems. These are later compared with our experimental results obtained in DNA hairpins. The general reader not interested in the mathematical details of the derivation can skip section 3.1.

3.1. Derivation of the equations

Let us consider a schematic version of our two-state system represented by a discrete spin variable σ that labels the state of the system, $\sigma = -1, 1$. The spin σ can switch between states of zero free energy ($\sigma = -1$) and free energy ΔG ($\sigma = 1$). The Hamiltonian of the system can be written as

$$H(\sigma) = \Delta G \frac{(\sigma + 1)}{2}. \tag{4}$$

In the presence of an external field f the Hamiltonian has a new term and is given by

$$H(\sigma) = \Delta G \frac{(\sigma + 1)}{2} - x_{\rm m} f \frac{(\sigma + 1)}{2}, \tag{5}$$

where $x_{\rm m}$ is the coupling between the system and the external field. For the case of the folding–unfolding reaction under force f, the two states, $\sigma = -1, 1$, correspond to the folded (F) and the unfolded (UF) states, respectively, and $x_{\rm m}$ is the molecular distance separating them along the reaction coordinate axis, i.e. $x_{\rm m} = x^{\rm F} + x^{\rm UF}$ (see figure 3).

We consider an isothermal perturbation where the external field is changed from an initial value $f_{\rm min}$ to a final one $f_{\rm max}$ following a given protocol $f(t)$, denoted as a ramping protocol. In this protocol the force is externally controlled and does not fluctuate. The equilibrium and thermodynamic properties that are computed when the force is controlled correspond to the so-called force ensemble.

According to the formalism of path thermodynamics introduced in [6], we consider a system composed of N independent two-state particles with dynamical evolution governed by the Hamiltonian in (5). A path or trajectory Γ of the system is defined by the sequence of configurations C_k, $\Gamma = \{C_k; 1 \le k \le N_{\rm s}\}$ with $C_k = \{\sigma_i^k, 1 \le i \le N\}$, the index k denoting a time equal to $k\Delta t$ where the total time $t_{\rm total}$ has been discretized in $N_{\rm s}$ steps of duration $\Delta t = t_{\rm total}/N_{\rm s}$. The work W per particle along a single path Γ is

$$W(\Gamma) = -\frac{x_{\rm m}}{2} \sum_{k=0}^{N_{\rm s}-1} m^{k+1}(f^{k+1} - f^k), \tag{6}$$

where $m^k = (1/N)\sum_{i=1}^{N} \sigma_i^k$ and f^k are the values of the magnetization and external field at time k. The factor $1/2$ in (6) arises from the absolute value of the change in extension associated with the transition $\sigma \to -\sigma$, $\Delta(x_{\rm m}\sigma/2) = x_{\rm m}$. On the other hand, the hopping

J. Stat. Mech. (2009) P02061

number M per particle over a single path is

$$M(\Gamma) = \frac{1}{N}\sum_{k=0}^{N_s-1}\sum_{i=0}^{N}\frac{1}{2}(1-\sigma_i^k\sigma_i^{k+1}). \tag{7}$$

The distribution of probability $P_N(\theta)$ for any observable θ (e.g. W or M) measured over all paths can be written as

$$P_N(\theta) = \sum_{\{\Gamma\}}\delta(\theta-\theta(\Gamma))P(\Gamma). \tag{8}$$

Assuming that the dynamics is Markovian, $P(\Gamma)$ is given by

$$P(\Gamma) = \left[\prod_{k=0}^{N_s-1}\prod_{i=1}^{N}q^k(\sigma_i^{k+1}\mid\sigma_i^k)\right]\prod_{i=1}^{N}p_o(\sigma_i^0), \tag{9}$$

where $q^k(\sigma'\mid\sigma)$ is the transition probability to go from σ to σ' at time k and p_o is the initial equilibrium distribution. The details for the computation of the average work and hopping number are presented in appendix A. Here, we outline the main steps of the computation and give the final results.

Following [6], we use the integral representation of the delta function and write the distribution of work and hopping number as $P_N(W) = \int \mathrm{d}\{\Gamma\}\mathrm{e}^{N\cdot a}$ and $P_N(M) = \int \mathrm{d}\{\Gamma\}\mathrm{e}^{N\cdot b}$, where a and b are functions defined over the space of trajectories $\{\Gamma\}$. In the thermodynamic limit ($N\to\infty$) the problem can be solved by applying the saddle point technique, i.e. maximizing the functions a and b with respect to their phase-space variables. From the saddle point equations we obtain closed expressions for the average quantities, $\langle\cdots\rangle$, where the brackets represent an average over an infinite number of realizations of the ramping protocol. In the continuous time limit, corresponding to $\Delta t\to 0$, $N_s\to\infty$ and $\Delta t\cdot N_s = t$, the average total work, $\langle W\rangle$, the average dissipated work, $\langle W_{dis}\rangle$, and the average hopping number, $\langle M\rangle$, are given by (see appendix A)

$$\langle W\rangle = -\frac{x_m}{2}\int_{f_{min}}^{f_{max}} m(f)\,\mathrm{d}f, \tag{10}$$

$$\langle W_{dis}\rangle = \langle W\rangle - W_{rev} = -\frac{x_m}{2}\int_{f_{min}}^{f_{max}}(m(f)-m_{eq}(f))\,\mathrm{d}f, \tag{11}$$

$$\langle M\rangle = \frac{1}{2r}\int_{f_{min}}^{f_{max}}(m(f)k_M(f)+k_T(f))(1/r(f))\,\mathrm{d}f, \tag{12}$$

where W_{rev} is equal to the reversible work, i.e. the work measured in the quasi-static limit. $k_{\rightarrow}(f)$ and $k_{\leftarrow}(f)$ are the kinetic rates corresponding to the transitions $\sigma=-1\to 1$ and from $\sigma=1\to -1$, respectively. $k_T(f), k_M(f)$ are defined as $k_T(f) = k_{\rightarrow}(f)+k_{\leftarrow}(f)$, $k_M(f) = k_{\rightarrow}(f)-k_{\leftarrow}(f)$. The functions $m_{eq}(f)$ and $m(f)$ are given by

$$m_{eq}(f) = \frac{k_M(f)}{k_T(f)}, \tag{13}$$

and

$$m(f) = m_{eq}(f) - \int_{f_{min}}^{f}\frac{\mathrm{d}m_{eq}(f_1)}{\mathrm{d}f_1}\exp\left[-\int_{f_1}^{f}\frac{k_T(f_2)}{r(f_2)}\,\mathrm{d}f_2\right]\mathrm{d}f_1, \tag{14}$$

where r is the loading rate defined as $r = \mathrm{d}f(t)/\mathrm{d}t$.

J. Stat. Mech. (2009) P02061

3.2. Constant loading rate

From now on we consider the case in which the force f is varied from $f_{\rm min}$ to $f_{\rm max}$ at a constant loading rate r. The initial and final values of the force, $f_{\rm min}$ and $f_{\rm max}$, are such that the equilibrium probabilities to be in the F state ($\sigma = -1$) are equal to 1 and 0, respectively, i.e. $m_{\rm eq}(f_{\rm min}) = -1$ and $m_{\rm eq}(f_{\rm max}) = 1$. Note that such a condition is always experimentally verified along the stretching process where initially the molecule is always folded and finally unfolded at the end of the process.

Interestingly, when the dynamics is governed by the rates in (2), $\langle W_{\rm dis}\rangle/k_{\rm B}T$ and $\langle M\rangle$ become functions of only two adimensional parameters, the fragility μ and an adimensional rate $\tilde{r}$:

$$\frac{\langle W_{\rm dis}\rangle}{k_{\rm B}T} = \int_{-\infty}^{\infty} {\rm d}x \int_{-\infty}^{x} {\rm d}y \, \frac{1}{\cosh^2 y} \exp\left(-\frac{1}{\tilde{r}} \int_{y}^{x} {\rm d}z \, {\rm e}^{\mu z} \cosh z\right), \tag{15}$$

$$\langle M\rangle = \frac{1}{2\tilde{r}} \left[\int_{-\infty}^{\infty} {\rm d}x \, (1 - \tanh^2 x) {\rm e}^{\mu x} \cosh x + \int_{-\infty}^{\infty} {\rm d}x \, {\rm e}^{\mu x} \sinh x \int_{-\infty}^{x} {\rm d}y \, \frac{1}{\cosh^2 y} \exp\left(-\frac{1}{\tilde{r}} \int_{y}^{x} {\rm d}z \, {\rm e}^{\mu z} \cosh z\right)\right]. \tag{16}$$

The fragility μ has been defined in (3) whereas the adimensional rate $\tilde{r}$ is given by

$$\tilde{r} = \frac{x_{\rm m} r}{k_{\rm c} 4 k_{\rm B} T}, \tag{17}$$

$k_{\rm c}$ being the folding–unfolding rate at the coexistence force value $f^{\rm c}$ at which the F and UF states are equally populated, $k_{\rm c} = k_{\rightarrow}(f_{\rm c}) = k_{\leftarrow}(f_{\rm c})$. Equation (15) is the equivalent of equation (49) in [6] obtained for the Glauber kinetics of a magnetic dipole in a magnetic field.

Since our goal is to identify relations between measurable quantities and the parameters characterizing the molecule, we have investigated the loading rate dependence of $\langle M\rangle$ and $\langle W_{\rm dis}\rangle$. In figure 4 we show the average dissipated work and the average hopping number as a function of the adimensional rate $\tilde{r}$ for different fragilities μ obtained by numerically integrating (15) and (16).

3.3. The stretching versus the releasing processes

Let us consider a symmetric protocol, i.e. in the stretching process the force f increases from $f_{\rm min}$ to $f_{\rm max}$ at a loading rate r, while in the releasing process f decreases from $f_{\rm max}$ to $f_{\rm min}$ at the same rate. According to (15) and (16) $\langle W_{\rm dis}\rangle$ and $\langle M\rangle$ are sole functions of $\tilde{r}, \mu$. The transformation from the stretching to the releasing force protocol (stretching/release transformation) corresponds to the exchange $x^{\rm F} \rightleftharpoons x^{\rm UF}$ implying $\mu \rightarrow -\mu$ in (15) and (16). Moreover, since r and $x_{\rm m}$ change sign under the stretch/release transformation, the parameter $\tilde{r}$ is invariant under such a transformation. For a given value of $\tilde{r}$ we can write

$$\langle W_{\rm dis}\rangle_{\rm S}(\mu) = \langle W_{\rm dis}\rangle_{\rm R}(-\mu), \qquad \langle M\rangle_{\rm S}(\mu) = \langle M\rangle_{\rm R}(-\mu). \tag{18}$$

Moreover it is easy to prove that the average hopping number $\langle M\rangle$ (16) is invariant under the transformation $\mu \rightarrow -\mu$, whereas the average dissipated work $\langle W_{\rm dis}\rangle$ (15) is not.

J. Stat. Mech. (2009) P02061

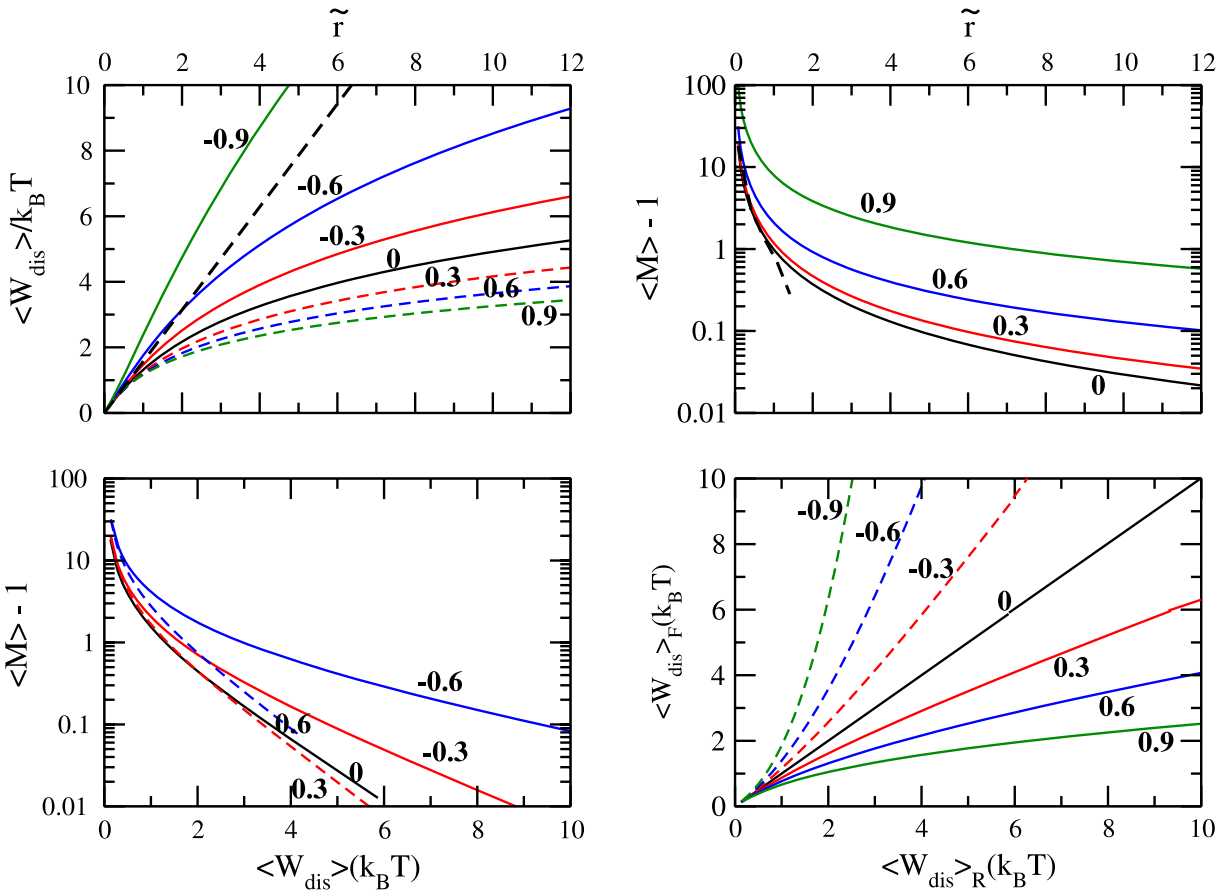

Figure 4. Various plots of $\langle W_{\rm dis}\rangle$ (in $k_{\rm B}T$ units) and $\langle M\rangle$ as a function of the adimensional loading rate $\tilde{r}$ obtained by numerically integrating (15) and (16) for various values of μ (indicated in the panels). (Top left) $\langle W_{\rm dis}\rangle_{\rm S}$ along the stretching process as a function of $\tilde{r}$. (Top right) $\langle M\rangle = \langle M_F\rangle = \langle M_R\rangle$ as a function of $\tilde{r}$ for both the stretching and releasing processes. The dashed line corresponds to the expansion (25) for $\mu = 0$. (Bottom left) $\langle M\rangle$ as a function of $\langle W_{\rm dis}\rangle_{\rm S}$ along the stretching process. (Bottom right) $\langle W_{\rm dis}\rangle_{\rm S}$ as a function of $\langle W_{\rm dis}\rangle_{\rm R}$. Note that $\langle W_{\rm dis}\rangle_{\rm S} < \langle W_{\rm dis}\rangle_{\rm R}$ for $\mu > 0$, $\langle W_{\rm dis}\rangle_{\rm S} > \langle W_{\rm dis}\rangle_{\rm R}$ for $\mu < 0$ whereas for $\mu = 0$ (TS located in the middle of the two states) $\langle W_{\rm dis}\rangle_{\rm S} = \langle W_{\rm dis}\rangle_{\rm R}$.

$\langle M\rangle(\mu)$ verifies

$$\langle M\rangle(\mu) \equiv \langle M\rangle_{\rm S}(\mu) = \langle M\rangle_{\rm S}(-\mu) = \langle M\rangle_{\rm R}(-\mu) = \langle M\rangle_{\rm R}(\mu). \tag{19}$$

This is a symmetry relation that can be checked in simulations and experiments. Results for $\langle W_{\rm dis}\rangle$ and $\langle M\rangle$ for different values of μ are shown in the top panels of figure 4.

In [22] (see the section *Fraction of trajectories that have at least one refolding* and appendix C) it was proven that the average fraction ϕ of trajectories (a quantity different from M) with more than one unfolding (refolding) (i.e. with $M \geq 3$) is equal along the stretching and release processes for a symmetric perturbation protocol. Although we have been unable to compute such a quantity ϕ using path thermodynamics it is interesting to see that the same symmetry relation (19) is also satisfied by the average hopping number $\langle M\rangle$.

In the numerical simulations done in [22] (see figure 11 in that reference) it was also shown that the fraction ϕ, when plotted as a function of the average dissipated work along the stretching process, $\langle W_{\rm dis}\rangle_{\rm S}$, collapses into a single curve for different two-state systems (i.e. that are characterized by different values of the parameters ΔG, $x^{\rm F}$, $x^{\rm UF}$ and $k_{\rm m}$). Although we cannot verify or falsify such a relation for ϕ, we can see that (19) precludes the validity of a similar relation for $\langle M\rangle$. As shown in the bottom left panel in figure 4, the relation between $\langle W_{\rm dis}\rangle_{\rm S}$ and $\langle M\rangle$ is not unique for different values of μ (otherwise $\langle W_{\rm dis}\rangle_{\rm S}(\mu)$ would be identical to $\langle W_{\rm dis}\rangle_{\rm R}(\mu)$, which we know is not generally true).

By applying (15) to the stretching and releasing processes it is possible to isolate the variable $\tilde{r}$ and express $\langle W_{\rm dis}\rangle_{\rm S}$ as a function of $\langle W_{\rm dis}\rangle_{\rm R}$ and the fragility μ. By plotting $\langle W_{\rm dis}\rangle_{\rm S}$ as a function of $\langle W_{\rm dis}\rangle_{\rm R}$ for different values of μ we can get *isofragility* curves that characterize the dissipation of the molecule along the stretching and releasing processes. The results are shown in the bottom right panel of figure 4. The relation between the dissipated work measured in the stretching and releasing processes can then be used to obtain information about μ, and hence about the TS of the folding/unfolding reaction.

3.4. Low loading rate regime

Equations (15) and (16) are not analytically integrable: however, we can solve them numerically as well as study their asymptotic behavior in the low loading rate regime. The low loading rate regime is investigated by expanding the expressions for $\langle W_{\rm dis}\rangle/k_{\rm B}T$ and $\langle M\rangle$, (15) and (16), around $\tilde{r}=0$. The analytical computation of the different terms of the expansion is presented in appendix B. We report the final result:

$$\frac{\langle W_{\rm dis}\rangle}{k_{\rm B}T} = \frac{\pi}{2}(1-\mu^2)\sec(\pi\mu/2)\tilde{r} - \frac{2}{3}\mu^2(1-\mu^2)\pi\csc(\pi\mu)\tilde{r}^2 + \tfrac{3}{40}(-5+51\mu^2-55\mu^4++9\mu^6)\pi\sec(3\pi\mu/2)\tilde{r}^3+\mathrm{O}(\tilde{r}^4), \tag{20}$$

$$\langle M\rangle = (\pi/2)\sec(\pi\mu/2)\frac{1}{\tilde{r}} + \frac{1}{48}(9-10\mu^2+\mu^4)\pi\sec(\pi\mu/2)\tilde{r} - \tfrac{1}{3}(\mu-\mu^3)\pi\csc(\pi\mu)\tilde{r}^2+\mathrm{O}(\tilde{r}^3). \tag{21}$$

The first term in the expansion of $\langle W_{\rm dis}\rangle$ agrees with the linear response result previously reported in [23] for the case $\mu =\!\!\rightarrow -1$ (i.e. $x^{\rm F}\to 0$, corresponding to an unfolding rate independent of force). For that case we get

$$\frac{\langle W_{\rm dis}\rangle}{k_{\rm B}T} = 2\tilde{r}+\mathrm{O}(\tilde{r}^2), \tag{22}$$

$$\langle M\rangle \to \infty, \tag{23}$$

whereas for the case $\mu=0$ (corresponding to a TS located in the middle between the F and UF states) we get

$$\frac{\langle W_{\rm dis}\rangle}{k_{\rm B}T} = \frac{\pi}{2}\tilde{r}+\mathrm{O}(\tilde{r}^2), \tag{24}$$

$$\langle M\rangle = \frac{\pi}{2\tilde{r}}+\mathrm{O}(\tilde{r}). \tag{25}$$

In figure 4 (top panels) we plot (black dashed lines) the expansion (24) (figure 4, top left panel) and the expansion (25) (figure 4, top right panel) for the case $\mu=0$.

4. Dissipation in the mixed ensemble

In the previous analysis we considered that the force is externally controlled and does not fluctuate (force ensemble). However, in the optical tweezers' experiments this is not the case because it is the position of the optical trap relative to the pipette (rather than the force) that is controlled. This corresponds to what has been called the mixed ensemble (see our companion paper [4]). The kinetic rates measured in the mixed ensemble are different from those measured in the force ensemble [24], [22, 25]–[27]. This is a consequence of the extreme sensitivity of the kinetic rates on height of the kinetic barrier (through the Arrhenius exponential dependence). Just a $\frac{1}{2}$ kcal mol^{-1} variation at room temperature in the value of the kinetic barrier can modify the rates by a factor of 2 (100%). Because the value of the kinetic rate k_c enters into the definition of the adimensional rate $\tilde{r}$ (17), a 100% variation in its value will invalidate an adequate comparison between theory and experiment. The influence of the ensemble on the kinetics is yet another example of nonequilibrium thermodynamics applied to small systems [2], i.e. about how nonequilibrium effects strongly depend on which experimental variables are controlled when the size of the system is small enough.

In the current theory the dissipated work and the average hopping number were obtained in the force ensemble. A path thermodynamics calculation for the mixed ensemble seems too tedious for the same analysis to be repeated again. In what follows we show that it is possible to carry over the theory in the mixed ensemble into the force-ensemble theory developed in section 3 just by appropriate rescaling of the kinetic rates (2) by a rescaling factor Ω. This rescaling only affects the value of the critical rate k_c that enters into the definition of $\tilde{r}$ (17) whereas the rest of the parameters (such as x_m and μ) remain unchanged.

4.1. A simple model for the mixed ensemble

Let us consider the system formed by a single hairpin in series with a Hookean spring (figure 5). The spring has stiffness equal to k_x whereas the molecule can be in two states, $\sigma = 0$ (folded) and $\sigma = 1$ (unfolded). This Hookean spring stands for the combined effect of the bead in the optical trap and the handles used to manipulate the hairpin. The total extension of the system is

$$\lambda = x + x_m\sigma, \tag{26}$$

where x is the extension of the spring and x_m is the molecular extension of the unfolded molecule. We will assume that x_m is not force-dependent and we will take a zero extension for the folded molecule.

In the mixed-ensemble protocol the total distance λ (equal to the distance between the optical trap and the micropipette) is controlled. The total energy of the system can be expressed as

$$E(\lambda, \sigma) = \tfrac{1}{2}k_x(\lambda - x_m\sigma)^2 + \sigma\Delta G, \tag{27}$$

where ΔG is the free energy difference between the unfolded and the folded states of the hairpin. The force–distance curve (FDC) is given by

$$f_\sigma(\lambda) = \frac{\partial E(\lambda, \sigma)}{\partial \lambda} = k_x(\lambda - x_m\sigma) = k_x x. \tag{28}$$

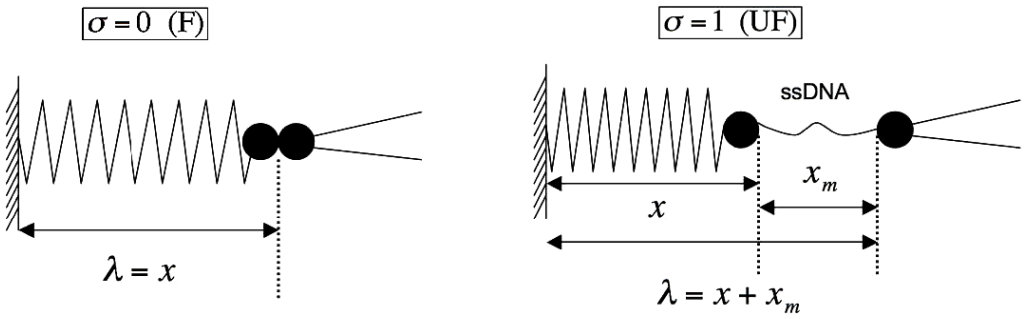

Figure 5. Schematic picture of a simple model for the mixed ensemble. (Left) Folded state $\sigma = 0$. (Right) Unfolded state $\sigma = 1$. See main text for the explanation of the different parameters.

The FDC of the system has two branches depending on whether the molecule is folded or unfolded. If the molecule is folded ($\sigma = 0$) we have

$$f_{\mathrm{F}}(\lambda) = \frac{\partial E(\lambda, 0)}{\partial \lambda} = k_x \lambda, \tag{29}$$

whereas in the other case

$$f_{\mathrm{UF}}(\lambda) = \frac{\partial E(\lambda, 1)}{\partial \lambda} = k_x(\lambda - x_{\mathrm{m}}), \tag{30}$$

i.e. both force–distance curves have the same slope (k_x), but there is a drop in the force equal to $k_x x_{\mathrm{m}}$ when the molecule unfolds. Note that this is exactly what is observed in the force-extension curves shown in figure 2.

What is the appropriate theory for the dissipated work in the mixed ensemble where the total distance (λ) rather than the force (f) is controlled? In principle we should expect work fluctuations to differ in both ensembles. The mechanical work along a trajectory Γ in the force and mixed ensemble, W_f and W_λ, respectively, is given by

$$W_f(\Gamma) = -x_{\mathrm{m}} \int_{f_{\min}}^{f_{\max}} \sigma \, \mathrm{d}f, \tag{31}$$

$$W_\lambda(\Gamma) = \int_{\lambda_{\min}}^{\lambda_{\max}} f \, \mathrm{d}\lambda. \tag{32}$$

$f_{\min}, f_{\max}$ ($\lambda_{\min}, \lambda_{\max}$) are the initial and final values of the force (total distance), the trajectory Γ is defined by the time evolution of $\{\sigma(t)\}$ and

$$x_{\mathrm{m}} = x^{\mathrm{F}} + x^{\mathrm{UF}}. \tag{33}$$

Integrating W_λ by parts and using the relations (28) and (26), we get

$$\begin{aligned} W_\lambda(\Gamma) &= [f(\lambda_{\max})\lambda_{\max} - f(\lambda_{\min})\lambda_{\min}] - \frac{1}{2k_x}[f^2(\lambda_{\max})^2 - f^2(\lambda_{\min})] - x_{\mathrm{m}} \int_{f(\lambda_{\min})}^{f(\lambda_{\max})} \sigma \, \mathrm{d}f \\ &= W_f(\Gamma) + (f_{\max}\lambda_{\max} - f_{\min}\lambda_{\min}) - \frac{1}{2k_x}(f_{\max}^2 - f_{\min}^2), \end{aligned} \tag{34}$$

where in the last line we have taken the instantaneous forces in the mixed ensemble equal to their values in the force ensemble, $f_{\min} = f(\lambda_{\min}), f_{\max} = f(\lambda_{\max})$. Although work distributions are expected to differ in both ensembles, differences in the average dissipated work are expected to be negligible. Therefore, $\langle W_\lambda^{\rm diss}(\Gamma)\rangle = \langle W_f^{\rm diss}(\Gamma)\rangle$ with $W_\lambda^{\rm diss}(\Gamma) = W_\lambda(\Gamma) - W_\lambda^{\rm rev}, W_f^{\rm diss}(\Gamma) = W_f(\Gamma) - W_f^{\rm rev}$. If the average dissipated work is the same in both ensembles then where is the expected difference between the measured dissipated work in the two experimental conditions (controlled f versus controlled λ)? The answer is in the kinetics. Because the kinetic rates in both ensembles are different, the ensemble of paths Γ generated in both ensembles have different work and dissipated work distributions.

4.2. Rescaling factor for the kinetic rates

Let us define $K_\rightarrow(\lambda), K_\leftarrow(\lambda)$ as the rates in the mixed ensemble (we use upper case letters to distinguish them from the force-ensemble rates). The mixed-ensemble rates must satisfy the detailed balance condition:

$$\frac{K_\rightarrow(\lambda)}{K_\leftarrow(\lambda)} = \exp(-\beta(E(\lambda,1) - E(\lambda,0))). \tag{35}$$

Inserting the expression for the energy (27) we get

$$\frac{K_\rightarrow(\lambda)}{K_\leftarrow(\lambda)} = \exp\left(-\beta\left(\frac{1}{2}k_x((\lambda - x_{\rm m})^2 - \lambda^2) + \Delta G\right)\right). \tag{36}$$

We can now express the difference of the squared terms in (36) as a product of a sum times a difference of two terms. However, according to the FDCs for the two branches (29) and (30), the factor 1/2 times the sum is just the λ-dependent average force $\bar{f}$ between the two branches:

$$\bar{f}(\lambda) = \tfrac{1}{2}(f_{\rm F}(\lambda) + f_{\rm UF}(\lambda)) = \tfrac{1}{2}k_x(2\lambda - x_{\rm m}). \tag{37}$$

Therefore

$$\frac{K_\rightarrow(\bar{f})}{K_\leftarrow(\bar{f})} = \exp[-\beta(-\bar{f}x_{\rm m} + \Delta G)], \tag{38}$$

where we parameterize the rates in the mixed ensemble $K_\rightarrow(\lambda), K_\leftarrow(\lambda)$ in terms of $\bar{f}$ rather than λ. Because these rates must satisfy detailed balance (38) we can write

$$K_\rightarrow(\bar{f}) = k_\rightarrow(\bar{f} + a), \tag{39}$$

$$K_\leftarrow(\bar{f}) = k_\leftarrow(\bar{f} + b), \tag{40}$$

where $k_\rightarrow, k_\leftarrow$ are the kinetic rates (2) and a, b are two arbitrary functions of $\bar{f}$ (i.e. of λ). Using the definitions (2) and inserting them in (38), we obtain the identity

$$ax^{\rm F} + bx^{\rm UF} = 0. \tag{41}$$

There is an infinite number of possible solutions that satisfy this equation. The most general solution is

$$a = Cx^{\rm UF}, \qquad b = -Cx^{\rm F}, \tag{42}$$

with C an arbitrary function of λ. We now express a, b in terms of the fragility μ defined in (3). It is straightforward to verify that

$$x^{\mathrm{F}} = \frac{\mu+1}{2}x_{\mathrm{m}}, \qquad x^{\mathrm{UF}} = \frac{1-\mu}{2}x_{\mathrm{m}}, \tag{43}$$

where we used (33). We now introduce the difference Δf between the forces along the F and UF branches at a given value of λ:

$$\Delta f = f_{\mathrm{F}}(\lambda) - f_{\mathrm{UF}}(\lambda) = k_x x_{\mathrm{m}}. \tag{44}$$

Note that in this simple model Δf is independent of λ (incidentally, let us note that the difference in force between the two branches shown in figure 2 is approximately constant). Inserting (43) and (44) into (42), we get

$$a = \alpha(1-\mu)\Delta f, \qquad b = -\alpha(1+\mu)\Delta f, \tag{45}$$

where α is a dimensionless constant. Substituting (45) into (39) and (40), we finally obtain

$$K_{\rightarrow}(\bar{f}) = k_{\rightarrow}(\bar{f} + \alpha(1-\mu)\Delta f), \tag{46}$$

$$K_{\leftarrow}(\bar{f}) = k_{\leftarrow}(\bar{f} - \alpha(1+\mu)\Delta f), \tag{47}$$

where α remains undetermined.

We cannot proceed further unless we introduce a microscopic model for the folding/unfolding of the hairpin in the proper experimental set-up. This was done in [22] where Kramers' theory was applied to investigate thermodynamic and kinetic aspects of RNA hairpins in the mixed ensemble relevant to pulling experiments using optical tweezers. The expression for the kinetic rates were obtained in formulae (B5) and (B6) in appendix B of that reference. These satisfy (46) and (47) with $\alpha = 1/4$. If we insert $\alpha = 1/4$ in (46) and (47) and use (2), we get

$$K_{\rightarrow}(\bar{f}) = k_{\rightarrow}(\bar{f}) \exp\left(\beta \frac{(1-\mu)}{4} x^{\mathrm{F}} \Delta f\right), \tag{48}$$

$$K_{\leftarrow}(\bar{f}) = k_{\leftarrow}(\bar{f}) \exp\left(\beta \frac{(1+\mu)}{4} x^{\mathrm{UF}} \Delta f\right). \tag{49}$$

Now we use again (43) to obtain

$$k_{\rightarrow}(\bar{f}) = \Omega K_{\rightarrow}(\bar{f}), \tag{50}$$

$$k_{\leftarrow}(\bar{f}) = \Omega K_{\leftarrow}(\bar{f}), \tag{51}$$

where Ω is a rescaling factor for the kinetic rates defined as

$$\Omega = \exp\left[-\left(\beta \frac{1-\mu^2}{8} x_{\mathrm{m}} \Delta f\right)\right], \tag{52}$$

showing that both rates $K_{\rightarrow}, K_{\leftarrow}$ must be rescaled with the same factor Ω.

J. Stat. Mech. (2009) P02061

4.3. The critical rate in the mixed ensemble, $\bar{k}_c$

We can now extend the theory developed for the force ensemble to the mixed ensemble. Instead of the simplified rates (2) we must use the rescaled rates (50) and (51). Consequently, all the results obtained in section 3 hold but by using the rates (50) and (51) instead of (2).

The value of the rates $K_{\rightarrow}(\bar{f}), K_{\leftarrow}(\bar{f})$ in the mixed ensemble can be measured in hopping experiments in the passive mode [26, 27]. In these experiments the total extension λ was held fixed and the evolution of the force is recorded. A typical passive mode force trajectory shows a square-like signal in which the force jumps between two values (see below in figure 6), the high value f_F corresponding to the F state and the low one f_{UF} corresponding to the UF state. Two types of representation for the passive rates were adopted in these references. In one representation rates are plotted as functions of $\bar{f}$ (or λ). These were called apparent rates, $K^{app}_{\rightarrow}(\bar{f}), K^{app}_{\leftarrow}(\bar{f})$, to distinguish them from *plain* passive rates where the relevant variable is the force corresponding to the folded or unfolded branches, f_F, f_{UF}, $K^{plain}_{\rightarrow}(f_F), K^{plain}_{\leftarrow}(f_{UF})$. The rates $K_{\rightarrow}, K_{\leftarrow}$ introduced in the previous section correspond to the apparent rates measured in passive hopping.

The value of the coexistence rate $\bar{k}_c$ that must be used in the definition of $\tilde{r}$ in (17) is given by

$$\bar{k}_c = k_{\rightarrow}(\bar{f}_c) = k_{\leftarrow}(\bar{f}_c), \tag{53}$$

and using the results (50) and (51) we have

$$\bar{k}_c = \Omega K^{app}_c, \tag{54}$$

where K^{app}_c is the critical apparent rate in the mixed ensemble defined as

$$K^{app}_c = K^{app}_{\rightarrow}(\bar{f}_c) = K^{app}_{\leftarrow}(\bar{f}_c), \tag{55}$$

where from (46), (47) and (2) we obtain $\bar{f}_c = f_c = \Delta G_1/x_m$.

By plotting the passive apparent rates as a function of $\bar{f}$ we can determine K^{app}_c as the value of the rate at which $K^{app}_{\rightarrow}(\bar{f})$ and $K^{app}_{\leftarrow}(\bar{f})$ intersect each other. The plain and the apparent rates satisfy

$$K^{app}_{\rightarrow}(\bar{f}) = K^{plain}_{\rightarrow}\left(\bar{f} + \frac{\Delta f}{2}\right), \tag{56}$$

$$K^{app}_{\leftarrow}(\bar{f}) = K^{plain}_{\leftarrow}\left(\bar{f} - \frac{\Delta f}{2}\right), \tag{57}$$

and from (50) and (51) we obtain

$$k_{\rightarrow}(\bar{f}) = \Omega K^{plain}_{\rightarrow}\left(\bar{f} + \frac{\Delta f}{2}\right), \tag{58}$$

$$k_{\leftarrow}(\bar{f}) = \Omega K^{plain}_{\leftarrow}\left(\bar{f} - \frac{\Delta f}{2}\right). \tag{59}$$

Finally, it is easy to verify that $K^{plain}_c = K^{app}_c \Omega^2$ and from (54) we get

$$\bar{k}_c = \frac{K^{plain}_c}{\Omega}. \tag{60}$$

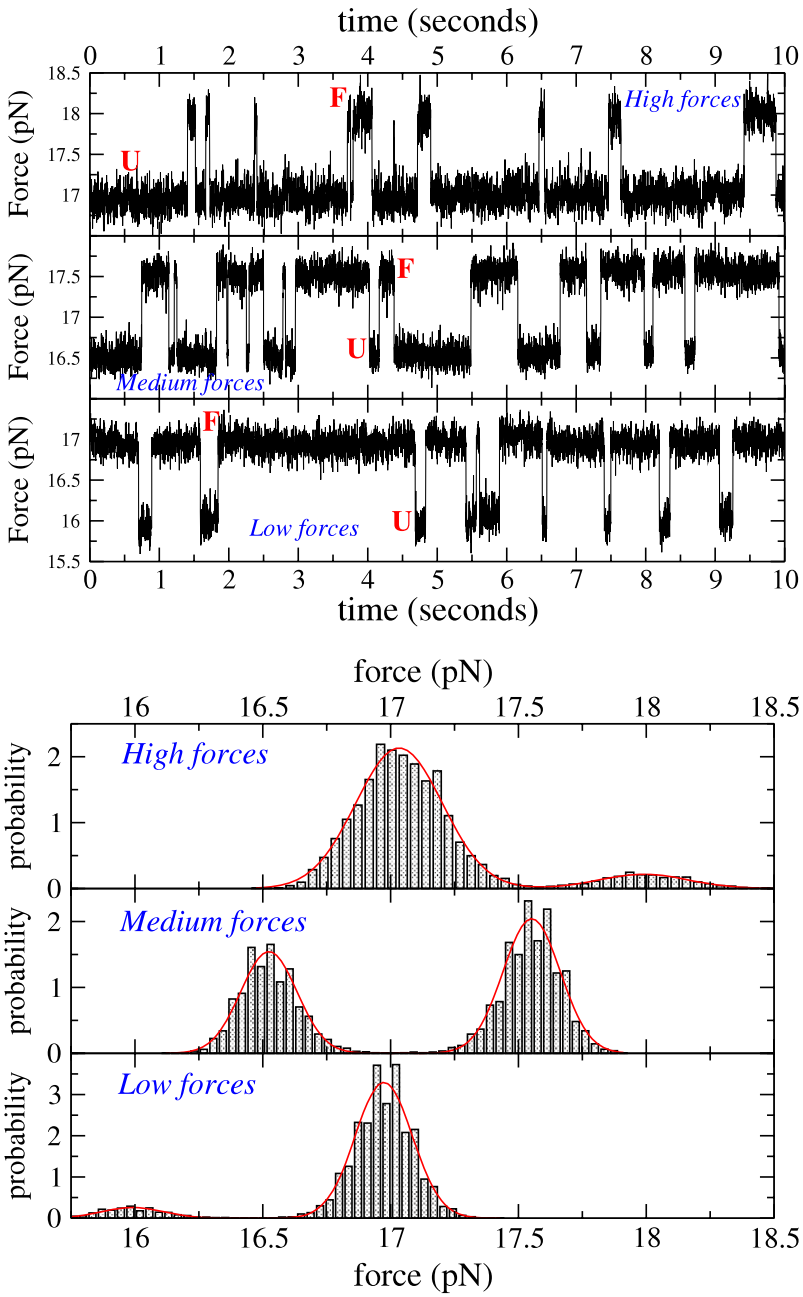

Figure 6. Hopping experiments in the passive mode. (Upper panel). A typical hopping trace measured at three trap positions: upper (high forces), middle (intermediate forces) and bottom (lower forces). (Lower panel) Force distributions for the dichotomic signal shown in the upper panel.

Because $\Omega < 1$ we have the following chain of inequalities:

$$K_{\rm c}^{\rm plain} < \bar{k}_{\rm c} < K_{\rm c}^{\rm app}. \tag{61}$$

Note that all these three rates are defined in the mixed ensemble and cannot be directly compared to experimental rates measured in hopping experiments carried out in the

constant force mode (i.e. in the force ensemble). The value of critical rate measured in hopping experiments in the constant force mode (what we called k_c in section 2 and is used in (15) and (16)) should be compared to pulling measurements of $\langle W_{\rm diss}\rangle$ and $\langle M\rangle$ done in the force ensemble, where the force acting on the bead (rather than the position of the trap) is controlled and ramped at a constant rate.

5. Experimental results

In this section we compare the experimental results for $\langle W_{\rm dis}\rangle$ and $\langle M\rangle$ that we obtained in pulling experiments for the DNA hairpin of figure 1(b) with the theoretical predictions developed in the preceding sections. Important parameters to compare theory and experiments are: the distances $x^{\rm F}$ and $x^{\rm UF}$, necessary to determine the fragility μ (3), and the coexistence rate, $\bar{k}_c$, necessary to determine the adimensional rate (17). A detailed characterization of the kinetics of a hairpin can be done with pulling or hopping experiments. In our companion paper [4] we investigated in detail the folding/unfolding kinetics of the hairpin using pulling experiments. However, accurate estimates for $\bar{k}_c$ are easier to obtain in hopping experiments. As we explained in section 4.3 the hopping experiments should be carried out in the passive mode [26, 27]. All experiments were done at a temperature 23–24 °C in a 1 M NaCl aqueous buffer with neutral pH (7.5) stabilized by tris HCl and 1 M EDTA.

5.1. Passive hopping experiments

Hopping experiments are useful to directly test the validity of the Kramers–Bell simplified kinetic rates (2) and extract kinetic parameters such as the coexistence rate $\bar{k}_c$ and the distances between the TS, and the F and U states, $x^{\rm F}$ and $x^{\rm UF}$. A typical hopping trace is shown in figure 6 (left panel). In the passive mode the trap is in a fixed position and the force switches between two values as the molecule executes transitions between the F and the UF states [26, 27]. A typical histogram of the forces is shown in figure 6 (right panel). By fitting the histograms to Gaussians, we can determine the average force in the F and UF states, $f_{\rm F}, f_{\rm UF}$, and the average force $\bar{f} = (f_{\rm F} + f_{\rm UF})/2$ for each passive mode configuration. From the dichotomic traces shown in figure 6 a we can also measure the residence times in the F and UF states for each trap position, $\tau_{\rm F}(\bar{f}), \tau_{\rm UF}(\bar{f})$. By averaging ($\langle\cdots\rangle$) the residence times we can extract the passive apparent rates:

$$K^{\rm app}_{\rightarrow}(\bar{f}) = \frac{1}{\langle\tau_{\rm F}(\bar{f})\rangle}, \qquad K^{\rm app}_{\leftarrow}(\bar{f}) = \frac{1}{\langle\tau_{\rm UF}(\bar{f})\rangle}. \tag{62}$$

The resulting rates are shown in figure 7. Linear fits to the logarithm of the rates give the following distances: $x^{\rm F} = 10.2$ nm and $x^{\rm UF} = 8.7$ nm. For the coexistence rate we obtain $K^{\rm app}_c = 2.3$ Hz with $\bar{f}_c \simeq 17.1$ pN, giving $x_{\rm m} = 18.9$ nm and $\mu = 0.1$. We also get $\Delta G = 78\ k_{\rm B}T$ ($k_{\rm B}T = 4.11$ pN nm). These values are compatible with those reported from rupture force kinetic studies in [4].

The critical rate $\bar{k}_c$ can then be extracted from the measured value for the passive rate $K^{\rm app}_c$ through (54) and the rescaling factor (52). To evaluate Ω we need to introduce the value for $\Delta f = f_{\rm F} - f_{\rm UF} \simeq 1.1$ pN and $k_{\rm B}T = 4.11$ pN nm. Substituting these numbers

J. Stat. Mech. (2009) P02061

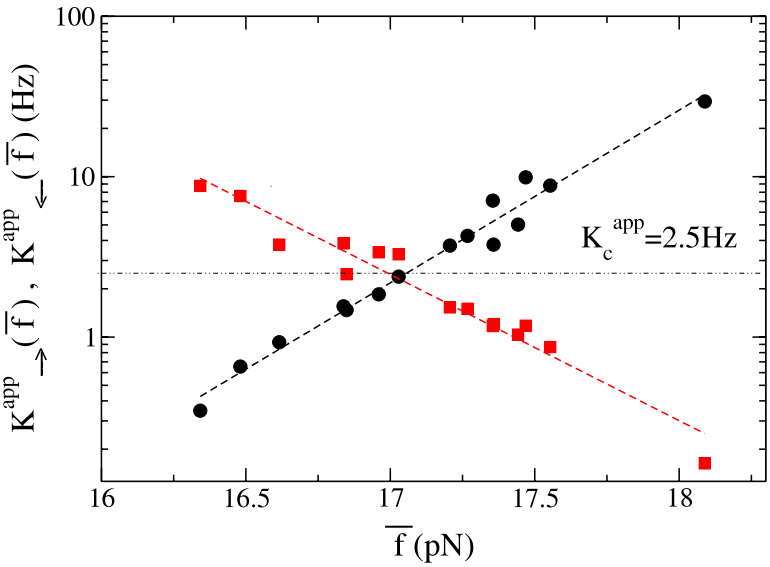

Figure 7. Determination of the critical rate in the passive mode. Rates in the passive mode as a function of the average force $\bar{f}$. The dashed lines are fits to the simplified rates (2). A least squares fit to the data gives $x^{\mathrm{F}} = 10.2$ nm, $x^{\mathrm{UF}} = 8.7$ nm, $\mu = 0.1, K_{\mathrm{c}}^{\mathrm{app}} = 2.5$ Hz. Data have been obtained for three molecules.

into (52) and (54), we get

$$\Omega = 0.54, \qquad \bar{k}_{\mathrm{c}} = 1.4 \text{ Hz}. \tag{63}$$

Note that from (60) we can also extract the value of $K_{\mathrm{c}}^{\mathrm{plain}}$. We obtain $K_{\mathrm{c}}^{\mathrm{plain}} = 0.74$. As expected, this agrees with the value of the critical rate found in the representation where rates are plotted as functions of the average force in the folded and unfolded state (data not shown). Finally, the value for $K_{\mathrm{c}}^{\mathrm{plain}}$ is not far from the value 0.58(1) reported from rupture force kinetic studies (see table 1 in [4]).

5.2. Pulling experiments: results for $\langle W_{\mathrm{dis}} \rangle$ and $\langle M \rangle$

To evaluate the average dissipated work and the average hopping number we have carried out pulling experiments on the sequence shown in figure 1(b) at five different pulling speeds (corresponding to five different loading rates ranging from 1 to 16 pN s^{-1}). A summary of the collected statistics and the results obtained for each molecule is shown in table 1.

By measuring the mechanical work and the hopping number along the stretching/releasing parts of each force cycle we have obtained the average total work and the average hopping number for each set of data. Finally, the average dissipated work for each molecule has been measured by subtracting the estimated reversible work from the average total work (how we estimated the reversible work is explained in our companion paper [4]).

In order to compare theory and experiments we take the following values obtained from the hopping experiments previously discussed in section 5.1: $x_{\mathrm{m}} = 19$ nm, $k_{\mathrm{B}}T = 4.11$ pN nm, $\mu = 0.1$ and $\bar{k}_{\mathrm{c}} = 1.4$ Hz.

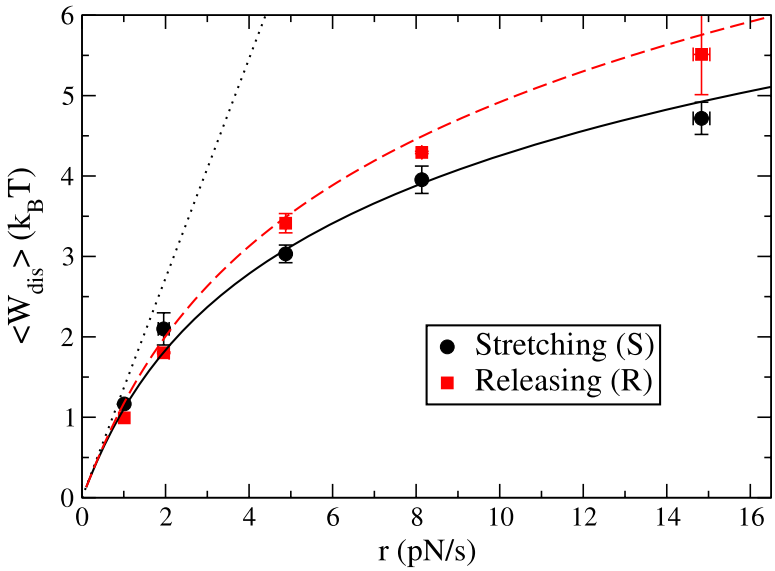

Figure 8. $\langle W_{\rm dis}\rangle$ for the stretching (circles) and releasing process (squares) plotted as a function of the loading rate. The continuous (dashed) lines are the analytical predictions (15) for the stretching (releasing) processes. The straight dotted line is the linear response regime (20).

Table 1. Collected statistics from pulling data. The parameters are: v (pulling speed in nm s^{-1}); r (loading rate in pN s^{-1}); $N_{\rm M}$ (total number of molecules); $N_{\rm S}$ (total number of stretchings); $N_{\rm R}$ (total number of releasings); $\langle W_{\rm dis}\rangle_{\rm S}$ (average dissipated work along the stretching process in $k_{\rm B}T$ units); $\langle W_{\rm dis}\rangle_{\rm R}$ (average dissipated work along the releasing process in $k_{\rm B}T$ units); $\langle M\rangle_{\rm S}$ (average hopping number along the stretching process); $\langle M\rangle_{\rm R}$ (average hopping number along the releasing process). The experimental errors are shown in parentheses and give an estimate of the variability among different molecules. (*) For the slowest pulls (25 nm s^{-1}) we have data for just one molecule so we do not indicate the experimental error.

v	r	$N_{\rm M}$	$N_{\rm S}$	$N_{\rm R}$	$\langle W_{\rm dis}\rangle_{\rm S}$	$\langle W_{\rm dis}\rangle_{\rm R}$	$\langle M\rangle_{\rm S}$	$\langle M\rangle_{\rm R}$
18.5	1.0	1	193	192	1.14(*)	1.00(*)	3.21(*)	3.13(*)
36.5	1.95	2	175	174	2.1(2)	1.80(1)	1.66(13)	1.70(9)
86.2	4.88	3	567	565	3.03(11)	3.41(12)	1.17(3)	1.11(3)
156	8.1	2	721	723	3.95(17)	4.29(2)	1.047(16)	1.080(6)
274.3	14.9	2	827	806	4.72(20)	5.5(5)	1.01(1)	1.04(2)

In figures 8–11 we show various plots of the average dissipated work and the average hopping number at five pulling speeds. The experimental results for the dissipated work are in agreement with the theory over a wide range of pulling speeds (figure 8). Moreover, the symmetry relation (19) seems reasonably well satisfied by the experimental data. The dependence of $\langle M\rangle$ on the loading rate is well reproduced by the theory (figure 9). The agreement is especially good in the right panel of figure 9 where the asymptotic large r region where $\langle M\rangle \to 1$ has been expanded by plotting $\langle M\rangle - 1$ on a logarithmic scale as a function of the loading rate r.

J. Stat. Mech. (2009) P02061

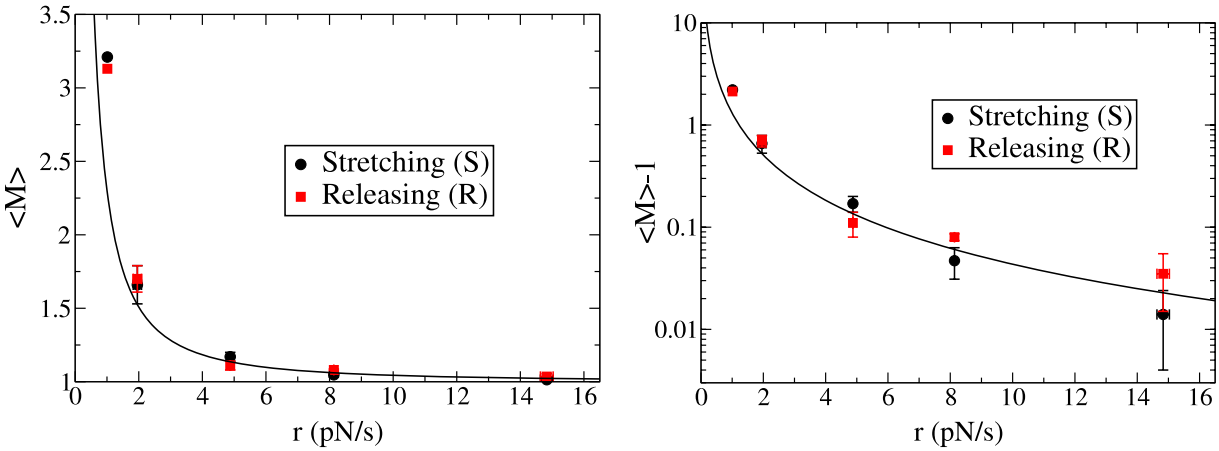

Figure 9. The average hopping number $\langle M \rangle$ for the stretching (circles) and releasing (squares) processes as a function of the loading rate. The continuous line is the analytical prediction (16) for the stretching and releasing processes that satisfy the symmetry relation (19). (Left panel) $\langle M \rangle$ in normal scale. (Right panel) To better appreciate the agreement between theory and experiments we plot the quantity $\langle M \rangle - 1$ on a logarithmic scale.

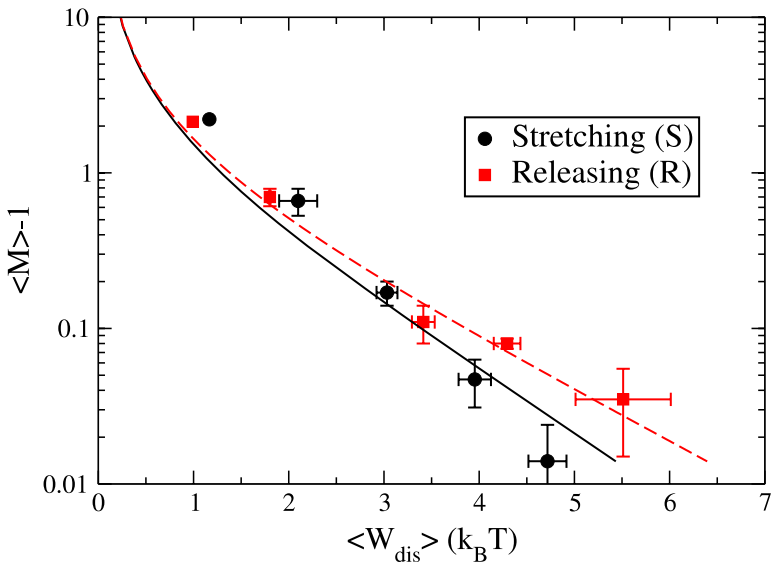

Figure 10. The average hopping number $\langle M \rangle$ as a function of $\langle W_{\rm dis} \rangle_{\rm S}$ and $\langle W_{\rm dis} \rangle_{\rm R}$ for the stretching (circles) and releasing (squares) processes.

Finally, in figure 10 we plot the average dissipated work as a function of the average hopping number whereas in figure 11 we plot the average dissipated work along the stretching process as a function of the average dissipated work along the release process. The plots shown in figures 10 and 11 have in common that they depend on the value of μ but not on $\bar{k}_{\rm c}$. Therefore, just by measuring $\langle W_{\rm dis} \rangle$ and $\langle M \rangle$ along the stretching and releasing processes we might be able to easily identify the value of the fragility of the molecule. The strong dispersion observed in the different *isofragility* lines shown

J. Stat. Mech. (2009) P02061

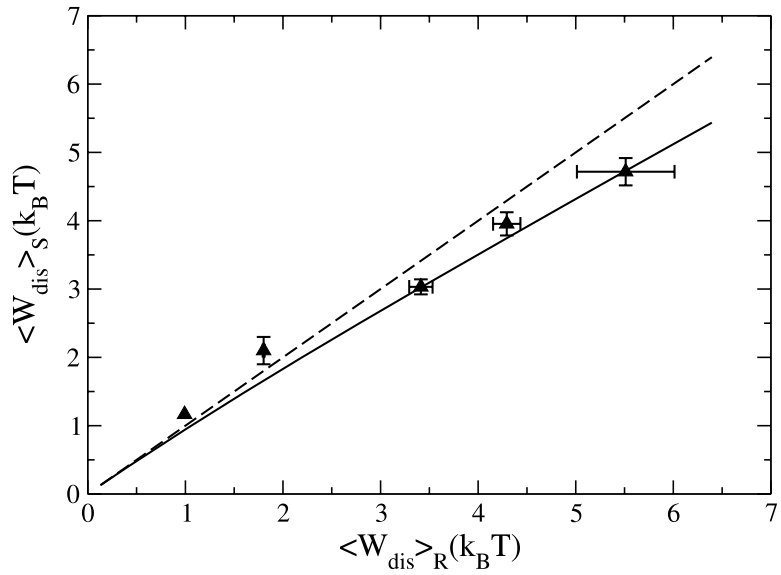

Figure 11. The average dissipated work $\langle W_{\rm dis}\rangle_{\rm S}$ as a function of $\langle W_{\rm dis}\rangle_{\rm R}$. The straight line corresponds to the case $\mu = 0$ that separates fragile and compliant behavior.

in figure 4 (left bottom panel), together with the unavoidable experimental errors in the data (see figure 10), preclude the use of a plot $\langle M\rangle$ versus $\langle W_{\rm dis}\rangle_{\rm S}$ to infer the value of μ. More convenient is the plot of $\langle W_{\rm dis}\rangle_{\rm S}$ versus $\langle W_{\rm dis}\rangle_{\rm R}$ where the *isofragility* lines change monotonically with μ (see figure 4, right bottom panel), making it easier to extract the value of μ from the experimental data (figure 11).

6. Conclusions

We have investigated irreversibility and dissipation effects in molecules that fold/unfold in a two-state manner under the action of mechanical force. We have developed a general theory for two-state molecules capable of predicting the average dissipated work and the average hopping number as a function of the loading rate and other parameters that describe the geometrical features of the free energy landscape of the molecule. The average dissipated work and the average hopping number are shown to depend on only two parameters: the fragility μ (which characterizes how brittle and compliant the molecular structure is) and the coexistence rate $\bar{k}_{\rm c}$ (measured at the coexistence force where the free energies of the folded and the unfolded states are equal). These two parameters can be experimentally measured in hopping experiments. We have tested the theory by carrying out pulling experiments on DNA hairpins using optical tweezers. We remark on two interesting results of the present work:

- *Rescaling of the kinetic rates.* We showed that in pulling experiments where the cantilever or the trap is moved at a constant pulling rate, the hopping rates measured from passive mode hopping experiments must be rescaled in order to account for the appropriate experimental conditions. The derivation of the rescaling factor Ω (52) shows the influence of the experimental set-up to quantify irreversibility effects in

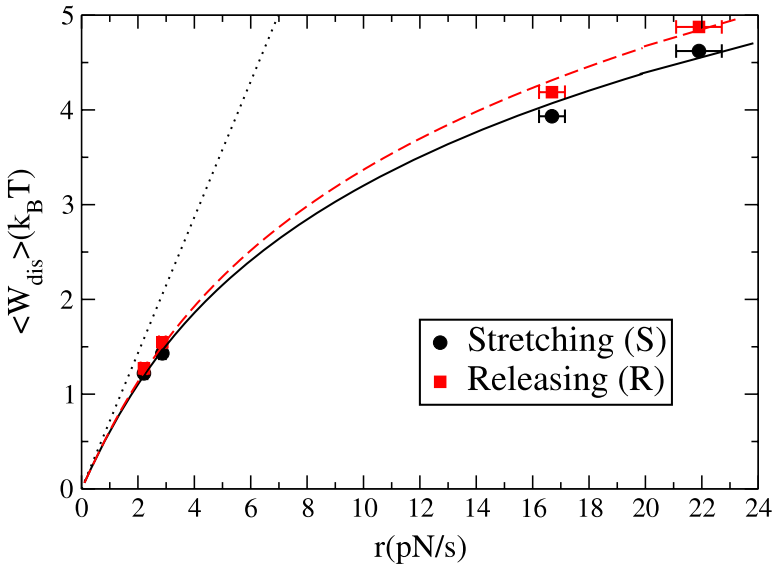

Figure 12. $\langle W_{\rm dis}\rangle$ for the stretching (circles) and releasing process (squares) plotted as a function of the loading rate in a 19 base pairs DNA sequence that was investigated [29] and with kinetics that deviates from perfect two-state behavior. The continuous (dashed) lines are the analytical predictions (15) for the stretching (releasing) processes. The straight dotted line is the linear response regime (20). The parameters for the simplified rates that are extracted from hopping experiments in the passive mode are: $x^{\rm F} = 9.53$ nm, $x^{\rm UF} = 9.00$ nm, $\Delta f = 1.0$ pN and $K_{\rm c}^{\rm app} = 4.4$ Hz. These parameters give $\mu = 0.02, \Omega = 0.57$ and $\bar{k}_{\rm c} = 2.5$ Hz.

small systems. In general, an accurate knowledge of the kinetic rates is not necessary in single-molecule studies (often, knowing the order of magnitude of the kinetic rate is enough). However, in our work it is necessary to determine the kinetic rates with high accuracy (let us say within 10%) in order to get an adequate comparison between theory and experiment. The rescaling factor Ω, albeit of order one, introduces an important correction that makes theory predictive in pulling experiments where the force is not controlled (e.g. in optical tweezers' or AFM experiments).

- *Symmetry property of hopping number.* The symmetry property for the average hopping number (19) appears as an interesting non-trivial consequence of the detailed balance property. We can define the distributions $p_{\rm S(R)}(M)$ for the fraction of trajectories with M transitions, $\langle M\rangle$ being just the first moment of the distributions. Is such a distribution identical for the stretching and releasing processes, $p_{\rm S}(M) = p_{\rm R}(M)$? A more elaborate theory, along the lines of the work recently developed by Chvosta and collaborators [28], might provide the answer to this question. Also it is interesting to speculate whether such a result holds in general reaction pathways beyond the two-state approximation.

The agreement found between theoretical predictions and experiments in DNA hairpins validates our theory and shows how this can be applied to infer kinetic information of the molecule under study. In general, the current theoretical results should be valid

J. Stat. Mech. (2009) P02061

for RNAs and proteins as well. However, many biomolecules do not fold in a two-state manner so the current theory should not be applicable to systems characterized by complex free energy landscapes, such as molecules with more than two states (e.g. molecules with intermediate or misfolded states) or even in two-state folders with many kinetic barriers. Yet we expect that the limits of applicability of the current theory should be flexible enough to describe a wide range of cases reasonably well. In figure 12 we compare the theory and the experiment for a 19 bps DNA sequence [4] that is not a faithful model of a two-state folder. The free energy landscape calculated for this molecule shows that the F and UF states are separated by two kinetic barriers [29]. Still, the theory applied to such a sequence agrees pretty well with the experiments. The extension of the current theory to more complex free energy landscapes as well as establishing limitations of the present theory remain as interesting open questions for future research.

Acknowledgments

We are grateful to Anna Alemany for a careful reading of the manuscript. We acknowledge financial support from grants FIS2007-61433, NAN2004-9348 and SGR05-00688.

Appendix A. Distribution of the work and the hopping number in a two-state system

We want to compute the distribution of probability of the work (6), and the hopping number (7), given by (8) and (9). We use the integral representation of the delta function, $\delta(x) = 1/2\pi \int_{-\infty}^{\infty} \mathrm{d}\lambda \, \exp(\mathrm{i}\lambda x)$, and introduce in (8) the following identity:

$$1 = \prod_{k=0}^{N_s-1} \frac{1}{2\pi} \int_{-\infty}^{\infty} \mathrm{d}\gamma^k \, \mathrm{d}m^k \exp\left[\mathrm{i}\gamma^k \left(m^k - \frac{1}{N}\sum_{i=1}^{N} \sigma_i^k\right)\right]. \tag{A.1}$$

After some manipulations, the distribution of any observable θ (e.g. work or hopping number) can be written as

$$P_N(\theta) \propto \int_{-\infty}^{\infty} \mathrm{d}\lambda \prod_{k=0}^{N_s-1} \mathrm{d}\gamma^k \, \mathrm{d}m^k \exp[N f_\theta(w, \lambda, \{\gamma^k\}, \{m^k\})], \tag{A.2}$$

where f_θ is a function that depends on the observable θ. We will use the notation $f_\mathrm{M} = a$ and $f_\mathrm{W} = b$ for the work and the hopping number, respectively. In the continuous limit the probability distribution (A.2) becomes a path integral, where the a and b functions are

$$a = -\lambda \left\{ W - x_\mathrm{m}/2 \left[(f_\mathrm{max} - f_\mathrm{min}) + \int_0^t \mathrm{d}s \, m(s) r(s) \right] \right\} + \tfrac{1}{2} \int_0^t \mathrm{d}s \{ m(s)[2\dot{\gamma}(s) + c(s)] + d(s) \} + \log[\mathrm{e}^{\gamma^0} k_\rightarrow(f_\mathrm{min}) + \mathrm{e}^{-\gamma^0} k_\leftarrow(f_\mathrm{min})], \tag{A.3}$$

$$b = -\lambda \frac{N}{2} + \frac{1}{2} \int_0^t \mathrm{d}s \, \{ m(s) \, [2\dot{\gamma}(s) + e(s)] + g(s) \} + \log[\mathrm{e}^{\gamma^0} k_\rightarrow(f_\mathrm{min}) + \mathrm{e}^{-\gamma^0} k_\leftarrow(f_\mathrm{min})]. \tag{A.4}$$

The function $r(s)$ is the rate of increasing the external field f, $r(s) = \mathrm{d}f/\mathrm{d}s$, and $f_{\min}$ is the initial value of the field in the ramping protocol. $k_{\rightarrow}$ and $k_{\leftarrow}$ are the rates (2) corresponding to the transition from $\sigma = -1$ to $\sigma = 1$ and from $\sigma = 1$ to $\sigma = -1$, respectively. The functions $c(s)$, $d(s)$, $e(s)$ and $g(s)$ are given by

$$c(s) = k_{\leftarrow}(f(s))(\mathrm{e}^{-2\gamma(s)} - 1) - k_{\rightarrow}(f(s))(\mathrm{e}^{2\gamma(s)} - 1), \tag{A.5}$$

$$d(s) = k_{\leftarrow}(f(s))(\mathrm{e}^{-2\gamma(s)} - 1) + k_{\rightarrow}(f(s))(\mathrm{e}^{2\gamma(s)} - 1), \tag{A.6}$$

$$e(s) = k_{\leftarrow}(f(s))(\mathrm{e}^{-2\gamma(s)+\lambda/2} - 1) - k_{\rightarrow}(f(s))(\mathrm{e}^{2\gamma(s)+\lambda/2} - 1), \tag{A.7}$$

$$d(s) = k_{\leftarrow}(f(s))(\mathrm{e}^{-2\gamma(s)+\lambda/2} - 1) + k_{\rightarrow}(f(s))(\mathrm{e}^{2\gamma(s)+\lambda/2} - 1), \tag{A.8}$$

with boundary conditions $\gamma(t) = 0$ and $m(0) = \tanh(\gamma(0) + \beta x_{\mathrm{m}} f_{\min}/2)$. Note that these boundary conditions break causality. In the large N approximation, the integral given by (A.2) can be estimated by using the saddle point technique. The saddle point equations, obtained by maximizing the a and b functions over the variables λ, $\gamma(s)$ and $m(s)$, are given by

$$\frac{\partial a}{\partial \lambda} = 0 = W - x_{\mathrm{m}}/2 \left[(f_{\max} - f_{\min}) - \int_0^t \mathrm{d}s\, m(s) r(s) \right],$$

$$\frac{\delta a}{\delta \gamma(s)} = 0 = \dot{m}(s) + m(s)\left[d(s) + k_{\mathrm{T}}(f(s))\right] + c(s) + k_{\mathrm{M}}(f(s)),$$

$$\frac{\delta a}{\delta m(s)} = 0 = -\frac{\gamma(s) x_{\mathrm{m}} r(s)}{2} + \dot{\gamma}(s) + \frac{c(s)}{2},$$

$$\frac{\partial b}{\partial \lambda} = 0 = \frac{N}{2} + \frac{1}{4}\int_0^t \mathrm{d}s \left\{ m(s)\left[e(s) + k_{\mathrm{M}}(f(s))\right] + g(s) + k_{\mathrm{T}}(f(s)) \right\},$$

$$\frac{\delta b}{\delta \gamma(s)} = 0 = \dot{m}(s) + m(s)\left[g(s) + k_{\mathrm{T}}(f(s))\right] + e(s) + k_{\mathrm{M}}(f(s)),$$

$$\frac{\delta b}{\delta m(s)} = 0 = \dot{\gamma}(s) + \frac{e(s)}{2},$$

where the dots mean the derivative with respect to time s and $k_{\mathrm{T}}(f), k_{\mathrm{M}}(f)$ are given by $k_{\mathrm{T}}(f) = k_{\rightarrow}(f) + k_{\leftarrow}(f)$, $k_{\mathrm{M}}(f) = k_{\leftarrow}(f) - k_{\rightarrow}(f)$. It can be shown [6] that the most probable value for the observable θ, θ^+, can be obtained as $(\partial f_\theta/\partial\theta)|_{\theta^+} = 0$, which gives $\lambda^+ = 0$. In the large N limit the most probable value and the average value coincide. The average work and hopping number are

$$\langle W \rangle = (x_{\mathrm{m}}/2)\left[(f_{\max} - f_{\min}) - \int_{f_{\min}}^{f_{\max}} m(f)\mathrm{d}f \right], \tag{A.9}$$

$$\langle M \rangle = (1/2)\int_{f_{\min}}^{f_{\max}} [m(f)k_{\mathrm{M}}(f) + k_{\mathrm{T}}(f)](1/r(f))\mathrm{d}f, \tag{A.10}$$

where the functions $m_{\mathrm{eq}}(f)$ and $m(f)$ are given by

$$m_{\mathrm{eq}}(f) = \frac{k_{\mathrm{M}}(f)}{k_{\mathrm{T}}(f)}, \tag{A.11}$$

and

$$m(f) = m_{\rm eq}(f) - \int_{f_{\rm min}}^{f} \frac{{\rm d}m_{\rm eq}(f_1)}{{\rm d}f_1} \exp\left[-\int_{f_1}^{f} \frac{k_{\rm T}(f_2)}{r(f_2)}\,{\rm d}f_2\right] {\rm d}f_1. \tag{A.12}$$

Appendix B. Expansion of the work and the hopping number in the low loading rate regime

For a system described by the folding and unfolding rates, $k_{\leftarrow}(f)$ and $k_{\rightarrow}(f)$, given in (2), the functions $k_{\rm T}(f)$ and $k_{\rm M}(f)$ are

$$k_{\rm T}(f) = k_{\leftarrow}(f) + k_{\rightarrow}(f) = 2k_{\rm c}{\rm e}^{-\beta\mu x}\cosh\, x, \tag{B.1}$$

and

$$k_{\rm M}(f) = k_{\leftarrow}(f) - k_{\rightarrow}(f) = 2k_{\rm c}{\rm e}^{-\beta\mu x}\sinh x, \tag{B.2}$$

where $k_{\rm c}$ is the folding or unfolding rate at the coexistence force $F^{\rm c}$, x corresponds to a dimensionless force $x = ((f - F^{\rm c})x_{\rm m})/2k_{\rm B}T$ and μ is defined as $\mu = (x^{\rm F} - x^{\rm UF})/x_{\rm m}$. Using these expressions we can write the average dissipated work and the average hopping number, (11) and (12), as

$$\langle W_{\rm dis}\rangle = k_{\rm B}T\int_{-\infty}^{\infty} {\rm d}x\, F(-\infty, x), \tag{B.3}$$

with

$$F(-\infty, x) = \int_{-\infty}^{x} {\rm d}y\, \chi_{\rm eq}(y){\rm e}^{-(\phi(y,x)/\tilde{r})}, \tag{B.4}$$

$$\langle M\rangle = \frac{1}{2\tilde{r}}\left[\int_{-\infty}^{\infty} {\rm d}x\, (-m_{\rm eq}^2(x) + 1){\rm e}^{-\beta\mu x}\cosh\, x + \int_{-\infty}^{\infty} {\rm d}x\, ({\rm e}^{-\beta\mu x}\sinh\, x)F(-\infty, x)\right], \tag{B.5}$$

where $\tilde{r}$ is a dimensionless loading rate, given by $\tilde{r} = (x_{\rm m}r/k_{\rm c}4k_{\rm B}T)$, the function $m_{\rm eq}$ (defined in (13)) is given by $m_{\rm eq}(x) = \tanh x$ and $\chi_{\rm eq}(x) = ({\rm d}m_{\rm eq}(x)/{\rm d}x) = 1/\cosh^2 x$. Finally, the function ϕ is given by $\phi(y, x) = -\int_y^x {\rm d}z\, k_{\rm T}(z)/2k_{\rm c} = \int_y^x {\rm d}z\, {\rm e}^{-\mu z}\cosh z$. Since $\phi(y, x)$ is defined positive for all $x \geq y$, when r goes to zero (or $\tilde{r} \to 0$) ${\rm e}^{-\phi(y,x)/\tilde{r}}$ vanishes except in $x = y$ where $\phi = 0$. Therefore, at the low loading rate regime, we can use a saddle point approximation and expand the integrand of $F(-\infty, x)$:

$$\begin{aligned} F(-\infty, x) = &\int_{-\infty}^{x} {\rm d}y \left[\chi_{\rm eq}(x) - \chi'_{\rm eq}(x)(y - x) + \frac{\chi''_{\rm eq}(x)(y - x)^2}{2} + \cdots\right] {\rm e}^{(-\phi'(x)(y-x)/\tilde{r})} \\ &\times \left[1 + \frac{\phi''(x)}{2\tilde{r}}(x - y)^2 - \frac{\phi'''(x)}{6\tilde{r}}(y - x)^3 + \cdots\right] \\ = &\tilde{r}\frac{\chi_{\rm eq}(x)}{\phi'(x)} + \tilde{r}^2\left[\frac{\phi''(x)\chi_{\rm eq}(x)}{\phi'(x)^3} - \frac{\chi'_{\rm eq}(f)}{\phi'(x)^2}\right] + \tilde{r}^3\left[-\frac{3\chi'_{\rm eq}(f)\phi''(x)}{\phi'(x)^4} + \frac{\chi''_{\rm eq}(f)}{4\phi'(x)}\right] \\ &+ {\rm O}(\tilde{r}^4), \end{aligned} \tag{B.6}$$

J. Stat. Mech. (2009) P02061

where the prime means the derivative with respect to x. By introducing the previous expansion to (B.4) and (B.5) we get

$$\begin{aligned}\beta\langle W_{\rm dis}\rangle &= A(\mu)\tilde{r} + B(\mu)\tilde{r}^2 + C(\mu)\tilde{r}^3 + \mathrm{O}(\tilde{r}^4),\\ \langle M\rangle &= \frac{\alpha(\mu)}{\tilde{r}} + \beta(\mu) + \gamma(\mu)\tilde{r} + \delta(\mu)\tilde{r}^2 + \mathrm{O}(\tilde{r}^3).\end{aligned} \tag{B.7}$$

The different coefficients of the expansion are given by

$$A(\mu) = -\int_{-\infty}^{\infty} \mathrm{d}x \frac{\mathrm{e}^{\mu x}}{\cosh^3 x} = \frac{\pi}{2}(1-\mu^2)\sec(\pi\mu/2), \tag{B.8}$$

$$B(\mu) = \int_{-\infty}^{\infty} \mathrm{d}x\, \mathrm{e}^{-2\mu x}\,\mathrm{sech}^4\, y(\mu + 3\tanh x) = \tfrac{-2}{3}\mu^2(1-\mu^2)\pi\csc(\pi\mu), \tag{B.9}$$

$$\begin{aligned}C(\mu) &= \int_{-\infty}^{\infty} \mathrm{d}x \frac{\mathrm{e}^{-3\mu x}}{\cosh^5 x}\left(\frac{-3}{\cosh^2 x} + 9\tanh^2 x + 4\mu\tanh x - \mu^2\right)\\ &= \tfrac{3}{40}(-5 + 51\mu^2 - 55\mu^4 + 9\mu^6)\pi\sec(3\pi\mu/2),\end{aligned} \tag{B.10}$$

$$\alpha(\mu) = \frac{1}{2}\int_{-\infty}^{\infty} \mathrm{d}x \frac{\mathrm{e}^{\mu x}}{\cosh x} = \frac{\pi}{2}\sec(\pi\mu/2), \tag{B.11}$$

$$\beta(\mu) = 0, \tag{B.12}$$

$$\begin{aligned}\gamma(\mu) &= 1/2\int_{-\infty}^{\infty} \mathrm{d}x\, \mathrm{e}^{-\mu x}\,\mathrm{sech}^3 x\tanh x(\mu + 3\tanh x)\\ &= \tfrac{1}{48}(9 - 10\mu^2 + \mu^4)\pi\sec(\pi\mu/2),\end{aligned} \tag{B.13}$$

$$\begin{aligned}\delta(\mu) = \frac{1}{2}\int_{-\infty}^{\infty} \mathrm{d}x \frac{\sinh x\,\mathrm{e}^{-2\mu x}}{\cosh^5 x}\Big(\frac{-3}{\cosh^2 x} +\\ + 9\tanh^2 x + 4\mu\tanh x - \mu^2\Big) = -1/3(\mu - \mu^3)\pi\csc(\pi\mu).\end{aligned} \tag{B.14}$$

References

[1] Ritort F, 2006 *J. Phys.: Condens. Matter* **18** R531 [arXiv:cond-mat/0609378]
[2] Bustamante C, Liphardt J and Ritort F, 2005 *Phys. Today* **58** 43
[3] Ritort F, 2008 *Adv. Chem. Phys.* **137** 31
[4] Mossa A, Manosas M, Forns N, Huguet J M and Ritort F, *Dynamic force spectroscopy of DNA hairpins: I. Force kinetics and free energy landscapes*, 2009 *J. Stat. Mech.* P02060
[5] Bustamante C and Smith S B, 2006 *US Patent Specification* 7,133,132, B2
[6] Ritort F, 2004 *J. Stat. Mech.* P10016
[7] Woodside M T, Behnke-Parks W M, Larizadeh K, Travers K, Herschlag D and Block S M, 2006 *Proc. Nat. Acad. Sci.* **103** 6190
[8] Jarzynski C, 1997 *Phys. Rev. Lett.* **78** 2690
[9] Crooks G E, 1999 *Phys. Rev.* E **60** 2721 [arXiv:cond-mat/9901352]
[10] Collin D, Ritort F, Jarzynski C, Smith S B, Tinoco I Jr and Bustamante C, 2005 *Nature* **437** 231
[11] Bonnet G, Krichevsky O and Libchaber A, 1998 *Proc. Nat. Acad. Sci.* **95** 8602
[12] Fernandez J M, Chu S and Oberhauser A F, 2001 *Science* **292** 653
[13] Hummer G and Szabo A, 2003 *Biophys. J.* **85** 5
[14] Li P T X, Collin D, Smith S B, Bustamante C and Tinoco I Jr, 2006 *Biophys. J.* **90** 250
[15] Liphardt D, Onoa B, Smith S B, Tinoco I Jr and Bustamante C, 2001 *Science* **292** 733

doi:10.1088/1742-5468/2009/02/P02061

J. Stat. Mech. (2009) P02061

[16] SantaLucia J Jr, 1998 *Proc. Nat. Acad. Sci.* **95** 1460
[17] Zuker M, 2003 *Nucleic Acids Res.* **31** 3406
[18] Leffer J E, 1953 *Science* **117** 340
[19] Hyeon C and Thirumalai D, 2005 *Proc. Nat. Acad. Sci.* **102** 6789
[20] Hyeon C and Thirumalai D, 2006 *Biophys. J.* **90** 3410
[21] Manosas M, Collin D and Ritort F, 2006 *Phys. Rev. Lett.* **96** 218301 [arXiv:cond-mat/0606254]
[22] Manosas M and Ritort F, 2005 *Biophys. J.* **88** 3224 [arXiv:cond-mat/0405035]
[23] Ritort F, Bustamante C and Tinoco I Jr, 2002 *Proc. Nat. Acad. Sci.* **99** 13544
[24] Gerland U, Bundschuh R and Hwa T, 2001 *Biophys. J.* **81** 1324 [arXiv:cond-mat/0101250]
[25] Gerland U, Bundschuh R and Hwa T, 2003 *Biophys. J.* **84** 2831 [arXiv:cond-mat/0208202]
[26] Wen J D, Manosas M, Li P T X, Smith S B, Bustamante C, Ritort F and Tinoco I Jr, 2007 *Biophys. J.* **92** 2996
[27] Manosas M, Wen J D, Li P T X, Smith S B, Bustamante C, Tinoco I Jr and Ritort F, 2007 *Biophys. J.* **92** 3010
[28] Subrt E and Chvosta P, 2007 *J. Stat. Mech.* P09019
[29] Unpublished results

J. Stat. Mech. (2009) P02061